



## OPEN

Strain glass transition in a multifunctional  $\beta$ -type Ti alloy

## SUBJECT AREAS:

METALS AND ALLOYS  
STRUCTURE OF SOLIDS AND LIQUIDS  
PHASE TRANSITIONS AND CRITICAL PHENOMENA  
MECHANICAL PROPERTIESYu Wang<sup>1</sup>, Jinghui Gao<sup>1</sup>, Haijun Wu<sup>1</sup>, Sen Yang<sup>1</sup>, Xiangdong Ding<sup>1</sup>, Dong Wang<sup>1</sup>, Xiaobing Ren<sup>1,2</sup>, Yunzhi Wang<sup>1,3</sup>, Xiaoping Song<sup>1</sup> & Jianrong Gao<sup>4</sup>

<sup>1</sup>Multi-disciplinary Materials Research Center, Frontier Institute of Science and Technology, MOE Key Laboratory for Nonequilibrium Synthesis and Modulation of Condensed Matter and State Key Laboratory for Mechanical Behavior of Materials, Xi'an Jiaotong University, Xi'an 710049, China, <sup>2</sup>National Institute for Materials Science, 1-2-1 Sengen, Tsukuba305-0047, Ibaraki, Japan, <sup>3</sup>Department of Materials Science and Engineering, The Ohio State University, 2041 College Road, Columbus, OH 43210, USA, <sup>4</sup>Key Lab of Electromagnetic Processing of Material, Northeastern University, 3-11 Wenhua Road, Shenyang 110004, China.

Received  
27 June 2013Accepted  
13 January 2014Published  
6 February 2014

Correspondence and requests for materials should be addressed to

X.B.R. (REN.

Xiaobing@nims.go.

jp); Y.Z.W. (wang.

363@osu.edu) or

X.P.S. (songxp@mail.

xjtu.edu.cn)

Recently, a class of multifunctional Ti alloys called GUM metals attracts tremendous attentions for their superior mechanical behaviors (high strength, high ductility and superelasticity) and novel physical properties (Invar effect, Elinvar effect and low modulus). The Invar and Elinvar effects are known to originate from structural or magnetic transitions, but none of these transitions were found in the GUM metals. This challenges our fundamental understanding of their physical properties. In this study, we show that the typical GUM metal Ti-23Nb-0.7Ta-2Zr-1.2O (at%) alloy undergoes a strain glass transition, where martensitic nano-domains are frozen gradually over a broad temperature range by random point defects. These nano-domains develop strong texture after cold rolling, which causes the lattice elongation in the rolling direction associated with the transition upon cooling and leads to its Invar effect. Moreover, its Elinvar effect and low modulus can also be explained by the nano-domain structure of strain glass.

The recent discovery of a new class of multifunctional Ti alloys<sup>1,2</sup> called GUM metals is challenging the conventional understanding of materials behavior. For example, these alloys yield at more than 20% of their ideal strength<sup>1</sup> while most materials yield at hundredths of their ideal strength. Except for high strength, they also exhibit superelasticity, high ductility and low modulus<sup>1</sup>. More interestingly, these alloys exhibit Invar and Elinvar effects<sup>1</sup> after heavy plastic deformation. The Invar effect and the Elinvar effect refer to that the thermal expansion coefficient of materials keeps near zero and the elastic modulus of materials maintains essentially a constant over certain temperature range respectively. These two effects have attracted long standing interests in practical and fundamental research, since they can be widely used in temperature sensitive device and high technology industry for avoiding unwanted thermal shock.

So far, many mechanisms such as dislocation-free deformation<sup>1,3-5</sup>, conventional dislocation plasticity<sup>6,7</sup>, twinning<sup>7</sup> and stress-induced martensitic transformation<sup>7-9</sup> were proposed to understand their unusual mechanical behaviors. However, few attempts were made and no model was proposed to understand comprehensively their Invar and Elinvar effects. Previous studies show that the Invar and Elinvar effects stem from structural or magnetic phase transition<sup>1,10,11</sup>. Nevertheless, it is surprising that there are no phase changes found in GUM metals within the temperature range where the two effects are displayed<sup>1</sup>. In this paper, we report that the typical GUM metal, Ti-23Nb-0.7Ta-2Zr-1.2O (at%) (TNTZ-1.2O) alloy actually undergoes a strain glass transition<sup>12-17</sup>, which accompanies the gradual freezing of martensitic nano-domains over a wide temperature range. Moreover, it will be shown that the existence of strain glass transition in the system is responsible for its Invar effect, Elinvar effect and low modulus.

The strain glass is formed by doping sufficient point defects into a normal martensitic system<sup>12-17</sup>. These point defects prevent the formation of long-range strain ordering by martensitic twin variants despite that such self-accommodating strain patterns are energetically more stable. Instead, randomly distributed nano-scale martensitic domains are formed due to the existence of point defects and frozen into a strain glass state. Unlike the martensitic transition, such a strain glass transition does not involve average structure change and proceeds gradually over a broad temperature range characterized by a broad storage modulus dip with obvious frequency dispersion around its freezing temperature  $T_g$ <sup>12</sup>. Furthermore, the kinetic freezing of strain glass is also characterized by a history dependent behavior in its thermal strain<sup>13</sup>, which is insensitive to cooling rate due to the diffusionless nature of the strain glass transition. It was further showed that the strain glass without exhibiting



spontaneous martensitic transition possesses unexpected shape memory effect and superelasticity, which is caused by stress induced strain glass to martensite transition<sup>15,16</sup>.

Recent intensive studies offer accumulating experimental observations, which show some interesting effects of GUM metals resemble the behaviors of strain glasses. For example, even though experimental observation shows that TNTZ-1.2O GUM metal does not undergo spontaneous martensitic transition<sup>15</sup>, its composition is close to that of the Ti-Nb-Ta-Zr-O martensitic alloy<sup>18</sup>. This is consistent with the fact that introducing more point defects will convert a normal martensitic system into a strain glass<sup>12-16</sup>. Moreover, the unexpected stress induced martensitic transition observed in the “non-martensitic” TNTZ-1.2O GUM metal<sup>7-9</sup> can be well explained by the stress induced strain glass to martensite transition<sup>15,16</sup>. All these clues indicate that a strain glass transition possibly occurs in the GUM metals. In the following, we will show the evidence of strain glass transition in TNTZ-1.2O GUM metal. Moreover, as exemplified by this system, our study also shows that strain glass transition serves as a new mechanism accounting for the Invar effect and Elinvar effect in materials.

## Results

Fig. 1(a) and 1(b) show the key experimental evidences for the existence of strain glass transition in the solution treated TNTZ-1.2O alloy, which was solution treated at 1273 K for 1 hour in vacuum and then quenched in water. As shown by the X-ray diffraction (XRD) profiles in Fig. 1(a), this solution treated sample shows no macroscopic crystal symmetry change and structure transition from 293 K to 123 K. However, its dynamically mechanical analysis (DMA) result (Fig. 1(b)) exhibits a broad storage modulus dip in this temperature regime, indicating the existence of a transition. Moreover, the frequency ( $\omega$ ) dispersion of its storage modulus dip temperature ( $T_g(\omega)$ ) obeys the Vogel-Fulcher relationship  $\omega = \omega_0 \exp[-E_a/k(T_g(\omega) - T_0)]$  (inset of Fig. 1(b)), which is the typical feature of strain glass<sup>12</sup>. Thus, these experimental results show that the solution treated TNTZ-1.2O alloy undergoes strain glass transition. Its ideal freezing temperature  $T_0$  is 188.2 K obtained by fitting the frequency dependent modulus dip temperatures with the Vogel-Fulcher relationship.

The formation of strain glass in TNTZ-1.2O alloy can be attributed to the doping of point defects into the normal Ti-Nb martensitic alloy. This can be revealed from the phase diagram in Fig. 1(d). The phase diagram is basically a Ti-Nb binary phase diagram, the transition temperatures of which are determined by DMA measurement of solution treated Ti-Nb based alloys. As shown in Fig. 1(d), when the content  $x$  of substitutional point defects, i.e., excess Nb atom in  $Ti_{100-x}Nb_x$  (abbreviated as Ti-xNb) is below 25, the Ti-Nb based system undergoes the spontaneous martensitic transition. The storage modulus dip temperature for the martensitic transition is independent on frequency, as shown by the DMA analysis of Ti-20Nb martensitic alloy in Fig. 1(c). The martensitic state is identified as the  $\alpha'$  martensite with an orthorhombic structure by XRD profile (inset of Fig. 1(c)). The martensitic transition temperature ( $M_s$ ) of the system is suppressed with increasing point defect content  $x$ . When the  $x$  is large than 25, the spontaneous martensitic transition of the Ti-Nb based martensitic system is suppressed completely and the system crossover into strain glass regime (Fig. 1(d)). Similarly, the formation of strain glass in the TNTZ-1.2O alloy is due to the doping of several kinds of point defects including substitutional (Nb, Ta, Zr) and interstitial (O) impurities into a binary Ti-20Nb martensitic alloy. The strain glass alloy exhibits frequency dependent behavior in its storage modulus dip (Fig. 1(b)) and an average BCC structure (Fig. 1(a)), being quite different from those of martensitic alloy (Fig. 1(c)). This demonstrates that the transforming properties of the system change significantly when the composition varies from martensitic to strain glass regime.

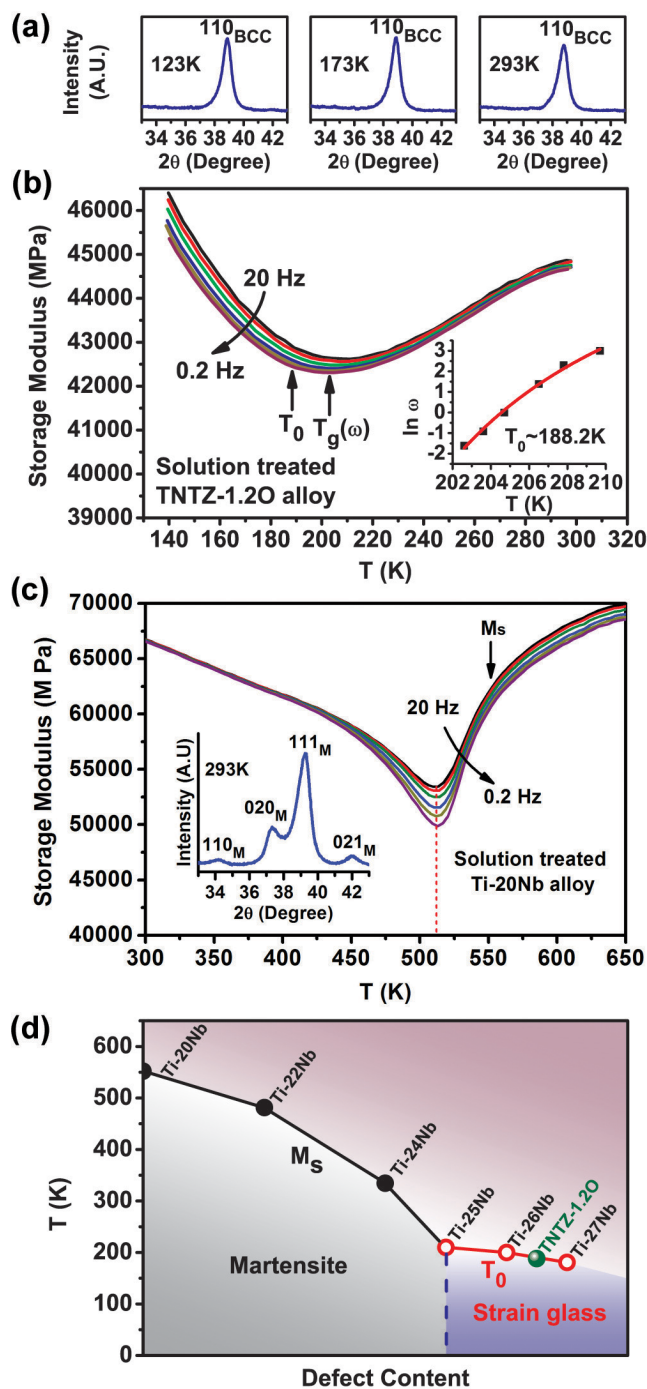


**Figure 1 | Evidence for existence of strain glass in solution treated TNTZ-1.2O alloy.** (a) Temperature dependence of XRD profile and (b) typical dynamic mechanical feature of strain glass for solution treated TNTZ-1.2O alloy. The inset of (b) shows that its storage modulus dip temperature ( $T_g(\omega)$ ) increases with increasing frequency ( $\omega$ ) obeying the Vogel-Fulcher relationship. (c) Dynamic mechanical feature of martensitic transition for solution treated Ti-20Nb alloy, which shows frequency independent behavior in its storage modulus dip temperature. The inset of (c) shows that the XRD profile of the martensite can be indexed by the orthorhombic  $\alpha'$  martensitic structure. (d) Strain glass phase diagram of Ti-Nb based alloy system, showing that the TNTZ-1.2O alloy can also be viewed as a Ti-Nb based strain glass.

It is reported that the Invar effect can be induced by cold rolling in GUM metal. To explore the origin of this effect, the thermal expansion (TE) behavior of the cold rolled TNTZ-1.2O samples with the 90% reduction in thickness and their corresponding solution treated

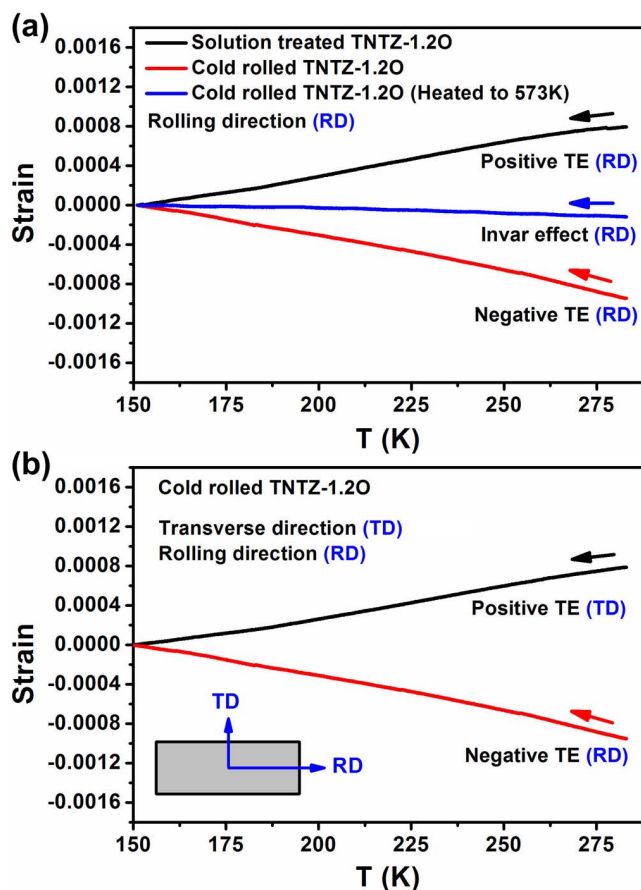


**Figure 2** | Thermal expansion behavior of solution treated and cold rolled TNTZ-1.2O strain glass. (a) The solution treated TNTZ-1.2O strain glass shows normal (positive) thermal expansion upon cooling from the initial temperature of 283 K to 150 K. However, the cold rolled TNTZ-1.2O sample shows negative thermal expansion upon cooling from 283 K to 150 K. When the cold rolled sample was heated to 573 K and then cooled down; it shows an Invar effect from 283 K to 150 K. (b) The cold rolled TNTZ-1.2O strain glass shows negative thermal expansion along rolling direction (RD) but positive thermal expansion along transverse direction (TD) upon cooling.

samples is measured by thermal mechanical analyzer (TMA). Fig. 2(a) shows that the solution treated sample exhibits normal thermal expansion along the rolling direction (RD) with decreasing thermal strain upon cooling from 283 K to 150 K. On the contrary, the cold rolled sample exhibits a negative thermal expansion along the RD when cooling from 283 K to 150 K. More interestingly, when the cold rolled sample was heated to 573 K and then cooled down, its thermal strain curve shows an invar effect from 283 K to 150 K. Similar result was also observed in an alloy of similar composition<sup>19</sup>. The big difference of thermal expansion behavior between solution treated and cold rolled TNTZ-1.2O strain glass demonstrates that cold rolling leads to the abnormal lattice expansion along RD on cooling. Moreover, cold rolling introduces strong anisotropy of the thermal expansion behavior of the cold rolled sample. As shown in Fig. 2(b), the cold rolled sample exhibits positive thermal expansion along transverse direction (TD, or orthogonal to the rolling direction (RD) as described above.

The microstructure of the solution treated TNTZ-1.2O alloy was characterized by transmission electron microscopy (TEM). Its bright field image (Fig. 3(a)) of  $[1\ 0\ 0]_{\text{BCC}}$  zone axis does not show any martensitic twin morphologies as observed in Ti-xNb ( $x < 25$ ) martensitic alloy<sup>20</sup>; only nano-sized domains of 10 ~ 20 nm can be recognized. The corresponding electron diffraction pattern in Fig. 3(b) exhibits BCC reflections being consistent with the XRD measurement. However, some weak and diffuse reflections (indicated by arrow) appear near  $(1/2\ 1/2\ 0)_{\text{BCC}}$  resembling the corresponding diffraction spots of orthorhombic  $\alpha''$  martensite<sup>21</sup>. Similarly, diffuse scattering spots also appears in the Fourier transform (Fig. 3(d)) of its high resolution TEM image (Fig. 3(c)). This indicates that there exist nano-scale local orthorhombic lattice domains. It was reported that the lattice correspondence between the orthorhombic  $\alpha''$  martensite and the BCC  $\beta$  parent phase is  $\alpha''[100]//\beta[100]$ ,  $\alpha''[010]//\beta[011]$ ,  $\alpha''[001]//\beta[0\bar{1}1]$ <sup>22,23</sup>. The lattice constants of  $\alpha''$  martensite,  $a$ ,  $b$ , and  $c$  (parallel to  $\alpha''[100]$ ,  $\alpha''[010]$  and  $\alpha''[001]$  respectively) and the lattice constant of the  $\beta$  parent phase,  $a_0$  (parallel to  $\beta[100]$ ), have the following relationship:  $a$  is smaller than  $a_0$ ,  $b$  is larger than  $\sqrt{2}a_0$  and  $c$  is slightly smaller than (essentially equal to)  $\sqrt{2}a_0$ <sup>23</sup>. The lattice correspondence between the local martensitic nano-domains and BCC matrix in this strain glass alloy should also share similar features, since its  $(1/2\ 1/2\ 0)_{\text{BCC}}$  diffuse scattering is similar to the corresponding diffraction spots of  $\alpha''$  martensite. In the

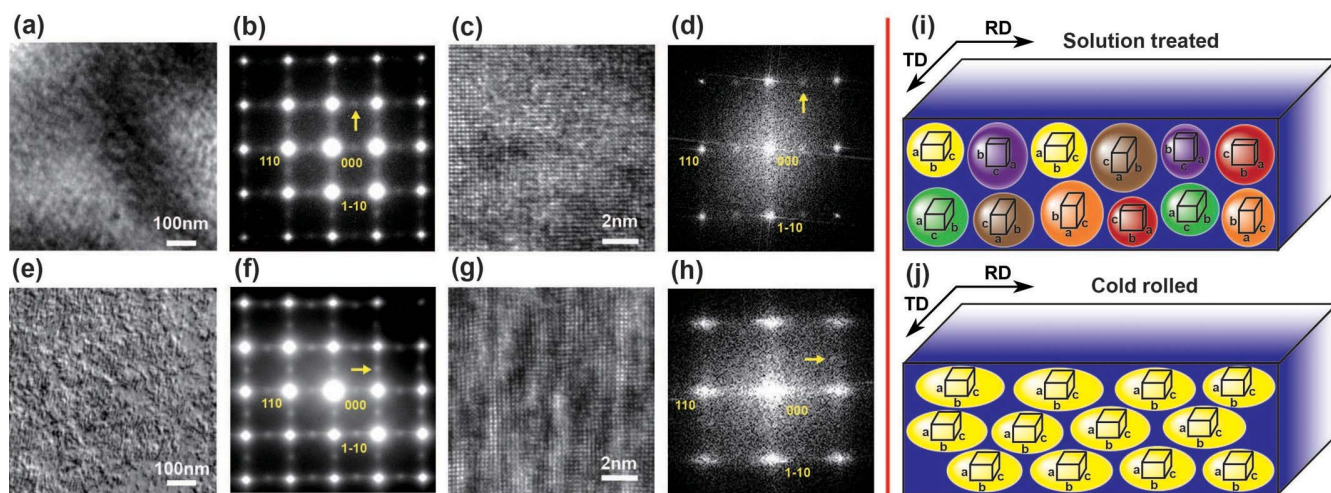


**Figure 3** | (a) The bright field image, (b) electron diffraction pattern, (c) HRTEM image and (d) Fourier transform of HRTEM image of  $[1\ 0\ 0]_{\text{BCC}}$  zone axis for solution treated TNTZ-1.2O strain glass alloy. (e) The bright field image, (f) electron diffraction pattern, (g) HRTEM image and (h) Fourier transform of HRTEM image of  $[1\ 0\ 0]_{\text{BCC}}$  zone axis for cold rolled sample. (i) and (j) show the schematic graph for the martensitic nano-domain structure in solution treated and cold rolled sample respectively.



solution treated TNTZ-1.2O alloy, the martensitic nano-domains of different orientation are distributed randomly in space as shown schematically in Fig. 3(i).

To understand the influence of cold rolling, the microstructure of the cold rolled TNTZ-1.2O alloy was also examined by TEM. The bright field image in Fig. 3(e) and high resolution TEM image in Fig. 3(g) show stripe-like nano-domains aligned parallelly, forming a sharp contrast to those of the solution treated sample. The Fourier transform (Fig. 3(h)) of the high resolution TEM image also shows spots elongated along the normal of the long axis of stripe modulations. However, its corresponding diffraction pattern (Fig. 3(f)) does not show any crystal symmetry change after cold rolling.

The sharp contrast of the nano-domain structures for the solution treated and cold rolled samples could be understood as follows. It was shown that cold rolling can induce preferred orientation variants of martensite (texturing) along the RD<sup>11,22</sup> to release the residual stress caused by the rolling<sup>11,24</sup>. Strong preferential formation of  $\alpha''$  martensite was also observed in cold rolled  $\beta$  Ti martensitic alloys, where the  $b$ -axis of the  $\alpha''$  martensite (which has a positive lattice misfit with its parent phase) is aligned along the RD and its  $a$ -axis (which has a negative lattice misfit with the parent phase) is aligned along the normal of the rolling plane<sup>22</sup>. It is reasonable to assume that cold rolling can also lead to similar texture for the martensitic nano-domains. As schematically shown in Fig. 3(j), the  $b$ -axis of the martensitic nano-domain is aligned along the RD and its  $a$ -axis is aligned to the normal of the rolling plane, which leads to the highly textured stripe-like nano-domain structure after cold rolling.

To explore the Elinvar effect of GUM metals, the temperature dependence of storage modulus of solution treated and cold rolled TNTZ-1.2O strain glass alloy was measured by DMA. As shown in Fig. 4, the solution treated sample exhibits a broad and shallow dip with a small variation in modulus during its strain glass transition. This forms a sharp contrast to the sharp and deep modulus dip during the martensitic transition<sup>25</sup> of the Ti-20Nb martensitic alloy, which is shown in the inset of Fig. 4. After cold rolling, the storage modulus curve of the TNTZ-1.2O strain glass changes essentially to a straight horizontal line (i.e., the Elinvar effect), which is similar to the experimental observation reported previously<sup>1</sup>.

## Discussion

The thermal expansion behavior of the solution treated and cold rolled TNTZ-1.2O alloy can be explained by the schematic drawings in Fig. 3(i) and 3(j). The thermal strain of TNTZ-1.2O strain glass

consists of two contributions. One is the normal thermal expansion stemming from anharmonic vibration of the crystal lattice. The other is the transformation strain originated from the growth of the martensitic nano-domains. For the solution treated sample, there is no preferred orientation of the martensitic nano-domains, as shown in Fig. 3(i). Thus on average the transformation strain of it is insignificant as compared to the normal thermal strain and it exhibits normal thermal expansion. However, for the cold rolled sample, the highly textured stripe-like nano-domains have their  $b$ -axis (along which there is a positive lattice mismatch) aligned along the RD, as shown in Fig. 3(j). When they grow upon cooling, the transformation strain causes an abnormal lattice expansion in the RD. Since the transformation strain along the  $b$ -axis of the martensitic lattice of nano-domain is larger than the normal thermal strain along the RD, the sample shows a negative thermal expansion on cooling from 283 K to 150 K. Moreover, the  $c$ -axis of the highly textured nano-domains (along which there is a slight negative lattice mismatch)<sup>23</sup> aligns along the TD (Fig. 3(j)), leading to the positive thermal expansion along TD. Such a strong anisotropy of thermal expansion between RD and TD demonstrates that the texture of nano-domains is developed in macro-scale for the cold rolled sample. When the cold rolled sample is heated to a higher temperature of 573 K, the residual stress due to cold rolling could be partially relaxed and the texture in the sample becomes weaker. Thus, the average transformation strain along the RD is reduced and becomes commensurate with the normal thermal strain, leading to the Invar effect.

The Elinvar effect observed in cold rolled TNTZ-1.2O alloy is also related with strain glass transition. Strain glass can be viewed as a composite system, in which two nano-scale “components”, parent matrix and martensitic nano-domains, coexist over wide temperature range from far above its ideal freezing temperature  $T_0$  to well below  $T_0$ <sup>12–14</sup>. The modulus of parent matrix decreases slowly but that of martensitic nano-domains increases slowly on cooling, which accompanies gradual volume fraction reduction of parent matrix and gradual volume fraction increase of martensitic nano-domains. The opposite contribution to elastic modulus of these two nano-scale “components” gives rise to a weak temperature dependence of modulus, i.e., broad and shallow modulus dip. Compared with the solution treated sample, the cold rolled TNTZ-1.2O alloy possesses more point defects, because vacancies and self-interstitials can be generated by cold rolling as proved by positron annihilation studies<sup>26</sup>. Recent experimental and theoretical studies<sup>17,27</sup> further reveal that the variation of volume fractions of martensitic nano-domains and parent matrix becomes much more sluggish by introducing more point defects. Thus, after cold rolling, the modulus reduction of the parent matrix and the modulus enhancement of martensitic nano-domains become smoother on cooling, resulting in extremely small variation of modulus with temperature, i.e., Elinvar effect.

Moreover, the low modulus of GUM metals could be explained from the view point of strain glass. During the strain glass transition, the BCC matrix undergoes local structure change and transforms into nano-sized orthorhombic martensitic domains. Thus there exists local structure instability in the system. It was shown that the structure instability of  $\beta$  Ti alloys can result in strong anisotropic elastic softening and leads to low modulus<sup>28,29</sup>. Similarly, the local structure instability in strain glass may result in local elastic softening as well, as revealed by the elastic softening measured by DMA and phonon softening detected by neutron scattering in strain glass composition<sup>27,30</sup>. This accounts for the low modulus value of GUM metals.

In conclusion, we found that the typical GUM metal, TNTZ-1.2O alloy, undergoes a strain glass transition, which is accompanied by gradual formation of martensitic nano-domains in a wide temperature range. The martensitic nano-domains with randomly distributed orientation in the solution treated TNTZ-1.2O strain glass alloy develop a strong texture after cold rolling. This leads to a negative

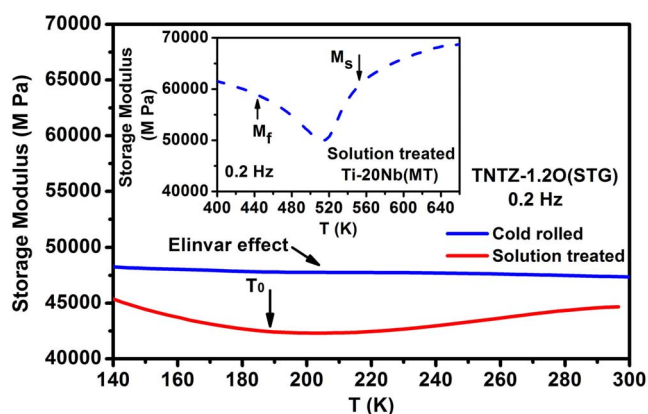


**Figure 4** | Temperature dependence of storage modulus for solution treated and cold rolled TNTZ-1.2O strain glass (STG) alloy. The inset shows the temperature dependence of storage modulus for the solution treated Ti-20Nb martensitic (MT) alloy, in which  $M_s$  is the starting temperature of martensitic transition and  $M_f$  is the finishing temperature of martensitic transition.



thermal expansion and the associated Invar effect. The Elinvar effect and low modulus are also related with the gradual formation of nano-sized martensitic domains.

## Methods

The Ti-Nb based alloy with the nominal composition of  $Ti_{100-x}Nb_x$  ( $x = 20-27$ ) and Ti-23Nb-0.7Ta-2Zr-1.2O (at %) (TNTZ-1.2O) were prepared by the arc melting method. The as cast ingots were solution treated at 1273 K for 2 h in evacuated quartz tubes and then quenched into water to obtain a homogenous supersaturated solid solution. Subsequently, the ingots were cold-rolled with the reduction of 90% in thickness. The cold rolled sheets are cut into pieces along rolling direction (RD) and transverse direction (TD, or orthogonal to the rolling direction) by an electro-discharge machine to obtain the cold rolled samples. To obtain the solution treated samples, some part of the cold rolled samples were solution treated again at 1273 K for 1 h in vacuum and then quenched into water. To prepare TEM samples, both the solution treated and the cold rolled samples were ground to less than 100  $\mu\text{m}$  thickness followed by punching into disks with diameter of 3 mm. Then, these disks were electro-polished in a solution of 6% perchloric acid, 35% butyl alcohol and 59% methanol (vol.%) at 253 K to 263 K and 10 V.

The AC storage modulus was measured with a dynamic mechanical analyzer (DMA) Q800 from TA Instruments. The measurement was performed on a single cantilever clamp with a continuous-cooling (cooling rate 2 K/min) multi-frequency (0.2 Hz–20 Hz) mode, which can record the storage modulus as a function of temperature and frequency simultaneously. The thermal expansion behavior is measured by thermal mechanical analyzer (TMA) 8310 from Rigaku Corporation with a very high strain resolution ( $\sim 10^{-6}$ ). The temperature change rate for TMA measurement is 2 K/min. The dependence of crystal structure on temperature was monitored by a Shimadzu X-ray diffractometer XRD-7000 with Cu-K $\alpha$  radiation. Before the XRD measurement at each temperature, 30 minutes were waited to ensure the temperature equilibrium of samples. The microstructures of the samples were observed by a transmission electron microscopy (TEM) JEOL JEM-2100F operating at 200 kV accelerating voltage.

- Saito, T. *et al.* Multifunctional Alloys Obtained via a Dislocation-Free Plastic Deformation Mechanism. *Science* **300**, 464–467(2003).
- Li, T., Morris, Jr., J. W., Nagasako, N., Kuramoto, S. & Chrzan, D. C. “Ideal” Engineering Alloys. *Phys. Rev. Lett.* **98**, 105503 (2007).
- Kuramoto, S., Furuta, T., Hwang, J. H., Nishino, K. & Saito, T. Plastic deformation in a multifunctional Ti-Nb-Ta-Zr-O alloy. *Metall. Mater. Trans. A* **37A**, 657–662(2006).
- Gutkin, M. Yu., Ishizaki, T., Kuramoto, S. & Ovid'ko, I. A. Nanodisturbances in deformed Gum Metal. *Acta Mater.* **54**, 2489–2499 (2006).
- Kuramoto, S., Furuta, T., Hwang, J., Nishino, K. & Saito, T. Elastic properties of Gum Metal. *Mater. Sci. Eng., A* **442**, 454–457(2006).
- Xing, H., Sun, J., Yao, Q., Guo, W. Y. & Chen, R. Origin of substantial plastic deformation in Gum Metals. *Appl. Phys. Lett.* **92**, 151905 (2008).
- Yang, Y., Li, G. P., Cheng, G. M., Li, Y. L. & Yang, K. Multiple deformation mechanisms of Ti-22.4Nb-0.73Ta-2.0Zr-1.34O alloy. *Appl. Phys. Lett.* **94**, 061901 (2009).
- Yang, Y. *et al.* Stress-introduced  $\alpha''$  martensite and twinning in a multifunctional titanium alloy. *Scripta Mater.* **58**, 9–12 (2008).
- Talling, R. J., Dashwood, R. J., Jackson, M. & Dye, D. On the mechanism of superelasticity in Gum metal. *Acta Mater.* **57**, 1188–1198(2009).
- Hausch, G., Bächer, R. & Hartmann, J. Influence of thermomechanical treatment on the expansion behavior of invar and superinvar. *Physica B* **161**, 22–24 (1989).
- Kainuma, R., Wang, J. J., Omori, T., Sutou, Y., & Ishida, K. Invar-type effect induced by cold-rolling deformation in shape memory alloys. *Appl. Phys. Lett.* **80**, 4348–4350(2002).
- Sarkar, S., Ren, X. & Otsuka, K. Evidence for strain glass in the Ferroelastic-Martensitic system  $Ti_{50-x}Ni_{50+x}$ . *Phys. Rev. Lett.* **95**, 205702 (2005).
- Wang, Y., Ren, X., Otsuka, K. & Saxena, A. Evidence for broken ergodicity in strain glass. *Phys. Rev. B* **76**, 132201 (2007).

- Wang, Y. *et al.* Evolution of the relaxation spectrum during the strain glass transition of  $Ti_{48.5}Ni_{51.5}$  alloy. *Acta Mater.* **58**, 4723–4729 (2010).
- Wang, Y., Ren, X. & Otsuka, K. Shape memory effect and superelasticity in a strain glass alloy. *Phys. Rev. Lett.* **97**, 225703 (2006).
- Wang, Y., Ren, X., Otsuka, K. & Saxena, A. Temperature-stress phase diagram of strain glass  $Ti_{48.5}Ni_{51.5}$ . *Acta Mater.* **56**, 2885–2896(2008).
- Wang, D., Wang, Y. Z., Zhang, Z. & Ren, X. Modeling Abnormal Strain States in Ferroelastic Systems: The Role of Point Defects. *Phys. Rev. Lett.* **105**, 205702 (2010).
- Furuta, T. *et al.* Mechanical properties and phase stability of Ti-Nb-Ta-Zr-O alloys. *Mater. Trans.* **48**, 1124–1130(2007).
- Nakai, M. *et al.* Anomalous Thermal Expansion of Cold-Rolled Ti-Nb-Ta-Zr Alloy. *Mater. Trans.* **50**, 423–426 (2009).
- Chai, Y. W., Kim, H. Y., Hosoda, H. & Miyazaki, S. Self-accommodation in Ti-Nb shape memory alloys. *Acta Mater.* **57**, 4054–4064 (2009).
- Semboshi, S., Shirai, T., Konno, T. J. & Hanada, S. In-situ transmission electron microscopy observation on the phase transformation of Ti-Nb-Sn shape memory alloys. *Metall. Mater. Trans. A* **39A**, 2820–2829(2008).
- Matsumoto, H., Watanabe, S. & Hanada, S. Beta TiNbSn alloys with low Young's modulus and high strength. *Mater. Trans.* **46**, 1070–1078(2005).
- Kim, H. Y. *et al.* Texture and shape memory behavior of Ti-22Nb-6Ta alloy. *Acta Mater.* **54**, 423–433(2006).
- Otsuka, K. & Wayman, C. M. *Shape Memory Materials* (Cambridge University Press, Cambridge, 1998).
- Schaller, R., Fantozzi, G. & Gremaud, G. *Mechanical Spectroscopy Q<sup>-1</sup> 2001*. (Trans Tech Publications, Zurich, 2001).
- Kwon, H. I. & Kim, I. S. A positron annihilation study of defects in extra high purity Ti with various deformation and annealing treatments. *Scripta Metall. Mater.* **32**, 607–610 (1995).
- Wang, D. *et al.* Strain glass in Fe-doped Ti-Ni. *Acta Mater.* **58**, 6206–6215 (2010).
- Kuramoto, S., Furuta, T., Nagasako, N. & Horita, Z. Lattice softening for producing ultrahigh strength of iron base nanocrystalline alloy. *Appl. Phys. Lett.* **95**, 211901 (2009).
- Ikehata, H. *et al.* First-principles calculations for development of low elastic modulus Ti alloys. *Phys. Rev. B* **70**, 174113 (2004).
- Fukuda, T., Choi, M., Kakeshita, T. & Ohba, T. Inelastic neutron scattering of a Ti-44 at.%Ni-6 at.%Fe alloy exhibiting an incommensurate-commensurate transition. *Mater. Sci. Eng. A* **481–482**, 235–238 (2008).

## Acknowledgments

The present work was financially supported by National Natural Science Foundation of China (Grant No. 51101118), National Basic Research Program of China (Grant Nos. 2012CB619401 and 2010CB631003), Natural Science Basic Research Plan in Shaanxi Province of China (Program No. 2013JQ6002), Program for New Century Excellent Talents, the Fundamental Research Funds for Central Universities of China, and the U.S. National Science Foundation DMR-1008349 (Yunzhi Wang).

## Author contributions

Yu W. performed all the experimental measurements. J.H.G. and H.J.W. helped with the TEM observation. S.Y., X.D.D., D.W. and X.P.S. helped with the results analysis. X.B.R. and Yunzhi W. designed the research project. J.R.G. provided the as-cast alloy samples. Yu W., X.B.R. and Yunzhi W. wrote the manuscript. All authors contributed to the discussions.

## Additional information

**Competing financial interests:** The authors declare no competing financial interests.

**How to cite this article:** Wang, Y. *et al.* Strain glass transition in a multifunctional  $\beta$ -type Ti alloy. *Sci. Rep.* **4**, 3995; DOI:10.1038/srep03995 (2014).



This work is licensed under a Creative Commons Attribution-NonCommercial-NoDerivs 3.0 Unported license. To view a copy of this license, visit <http://creativecommons.org/licenses/by-nc-nd/3.0>